*J Mater Sci* (2019) 54:10119–10129

Ceramics

# High-strength macro-porous alumina ceramics with regularly arranged pores produced by gel-casting and sacrificial template methods

Mengwen Zhang[1,2], Xiaodong Li[1], Mu Zhang[1,*], Zhimeng Xiu[1], Ji-Guang Li[3], Junpeng Li[4], Ming Xie[4], Jialin Chen[4], and Xudong Sun[1,2,*]

[1] *Key Laboratory for Anisotropy and Texture of Materials (Ministry of Education), School of Materials Science and Engineering, Northeastern University, Shenyang 110819, China*

[2] *Liaoning Engineering Laboratory of Special Optical Functional Crystals, College of Environmental and Chemical Engineering, Dalian University, Dalian 116622, China*

[3] *Research Center for Functional Materials, National Institute for Materials Science, Namiki 1-1, Tsukuba, Ibaraki 305-0044, Japan*

[4] *State Key Laboratory of Advanced Technologies for Comprehensive Utilization of Platinum Metals, Kunming Institute of Precious Metals, Kunming 650106, China*

**Received:** 28 December 2018
**Accepted:** 27 March 2019
**Published online:** 11 April 2019



## ABSTRACT

Macro-porous alumina ceramics were prepared by the gel-casting method using sacrificial polystyrene spheres as the template. The resulted porous alumina ceramics have regularly arranged pores and high cell wall densities, which confer high mechanical strength to the porous ceramics. The highest compressive strength for a porous alumina ceramic, with a relative density of 30%, in this work is 28 MPa, which is at least 74% higher than that of previously reported porous alumina ceramics with the same porosity. The results show that the cell wall density, window size and cell size can be adjusted by controlling the sintering temperature, solid loading percentage of the alumina slurry and the size of the polystyrene spheres. With the increase in cell wall density and decrease in cell size and window size, the compressive strength of the porous alumina increases. Thus, a novel porous structure with high porosity and high strength can be made by this flexible method which is also suitable for making complicated shapes and large sizes.

## Introduction

Due to their high porosity, large specific surface area, lightweight, low thermal conductivity, high-temperature mechanical strength and good chemical inertness, macro-porous alumina ceramics are extensively used as bone tissue scaffolds [1], filters [2], thermal insulators [3], catalyst carriers [4], hot-gas collectors [5] and sound absorbers [6]. It should be noted that porous ceramic components are frequently

Address correspondence to E-mail: zhangm@smm.neu.edu.cn; xdsun@mail.neu.edu.cn

https://doi.org/10.1007/s10853-019-03576-8

subjected to mechanical loads in their numerous applications, and good structural reliability is critically needed [7, 8].

Various synthetic methods have been successfully employed to prepare macro-porous alumina ceramics, including partial sintering, replica templating, direct foaming and sacrificial templating [9]. The porous ceramics made by partial sintering can achieve high strength [10], but these pore sizes are only in the range of several micrometres, and the porosity is often less than 60% [11–13]. The typical flaws of the strut walls formed upon pyrolysis of the template in the replica template method can markedly degrade the final mechanical strength of the porous ceramics [14]. Although dip-coating and re-sintering procedures have been developed, unfortunately, the compressive strength of porous alumina made by these methods is still less than 1 MPa [15]. Porous ceramics prepared by direct foaming displayed inhomogeneous pore distribution and pore sizes [1, 16, 17]. A porous mullite ceramic prepared by foaming coupled with gel casting showed a deviation of 300 μm in the pore sizes [18]. The sacrificial template method can easily control the pore size, pore shape and porosity. However, it has been reported that as the porosity increased from 60 to 70%, the strength largely decreased from 24.4 to 3.7 MPa [19]. It is worth mentioning that freeze-casting is a special sacrificial template method to obtain porous alumina [20]. Although the structures are anisotropic, porous ceramics prepared by freeze-casting can achieve very high compressive strength. Chen et al. [21] reported that a 150 MPa compressive strength has been achieved by freeze-casted porous alumina ceramics at 42% porosity. However, the pore size of the porous ceramics made by freeze-casting is often less than 100 μm. Despite these studies and the results obtained, the manufacturing of macro-porous alumina ceramics with both high porosity and high mechanical strength is still a difficult problem.

Carefully tailored porous structures have great potential to give rise to ceramics with substantially improved strength [22]. This is potentially attained by more precisely controlling the pore characteristics themselves, such as size, shape and distribution [12, 23]. Porous ceramics with a reverse opal structure showed unique advantages [24, 25]. However, there are limited reports on the mechanical properties of these porous materials that possess micrometre or even millimetre-sized pores. Alumina ceramic foams with adjustable cell structure have been fabricated by centrifugal slip casting in pre-arrayed epispastic polystyrene templates, but the compressive strength of this porous alumina, with 75% porosity, only achieved a value of 3.2 MPa [26]. Moreover, it is difficult to avoid segregation in the centrifugal process, and the shape of the samples is also limited. As a result, exploring the mechanical properties of porous ceramics with large pore sizes and tailored inverse opal structures remains an interesting challenge.

In this work, a combined gel-casting and sacrificial template method was developed to prepare porous alumina ceramics with high porosity and high strength. The sacrificial templates are isometric polystyrene spheres, which can be almost closely packed by self-assembly, providing regularly arranged arrays. Then, an alumina slurry was used to fill the interstitial space by gel casting, guaranteeing a highly dense strut. Moreover, the gel-casting method is suitable for making samples of large size. Thus, the influence of sintering temperature, solid loading percentage of the alumina slurry and polystyrene sphere size on the pore structure, physical properties and mechanical properties of the porous alumina ceramics were studied.

## Experimental procedures

### Raw materials

Commercial α-alumina (2 μm, Zibo Aotai New Material Technology Co., Ltd., China) was used to prepare the porous ceramics, and polystyrene spheres (Gongyi Xinjiayuan Water Treatment Materials Co., Ltd., China) with different sizes were chosen as the sacrificial templates. Aqueous gel casting was carried out by utilizing methacrylamide (MAM, $C_4H_7NO$, ≥ 98% purity, Sinopharm Chemical Reagent Co., Ltd., China), *N*,*N*′-methylenebisacrylamide (MBAM, $C_7H_{10}N_2O_2$, ≥ 98% purity, Sinopharm Chemical Reagent Co., Ltd., China), ammonium persulfate (APS, $N_2H_8S_2O_8$, ≥ 98% purity, Sinopharm Chemical Reagent Co., Ltd., China) and *N*,*N*,*N*′,*N*′-tetramethylethylenediamine (TEMED, $C_6H_{10}N_2$, ≥ 98% purity, Sinopharm Chemical Reagent Co., Ltd., China) as the monomer, cross-linker, initiator and catalyst, respectively. Among these, the concentrations of APS and TEMED were diluted

to 10 wt% and 50 vol%, respectively. Moreover, ammonium citrate ($C_6H_{17}N_3O_7$, ≥ 98.5% purity, Tianjin Kemiou Chemical Reagent Co., Ltd., China) and ethyl alcohol (≥ 99.7% purity, Sinopharm Chemical Reagent Co., Ltd., China) were used as the dispersant and wetting agent, respectively.

## Preparation of the porous alumina ceramics

The process flowchart for preparing the porous alumina ceramics by the gel-casting and sacrificial template methods is shown in Fig. 1, and the compositions of the alumina slurries with different solid loading percentages are shown in Table 1. The slurry, containing alumina powder, solvent, monomer, cross-linker and dispersant, was mixed by ball milling for 24 h, with the weight ratio of milling balls to alumina powder being 2:1, followed by a vacuum stirrer for 30 min to remove bubbles produced during ball milling. Then, the wetting agent, catalyst and initiator were added to the slurry accompanied by magnetic stirring. Soon afterwards, the alumina slurry was poured into a mould that had been filled with close-packed polystyrene spheres. The polystyrene spheres were packed by self-assembly performance and mechanical vibration, and its packing density is 69.3%. After the polymer had cross-linked and the slurry had solidified under ambient conditions for 12 h, the samples were carefully removed from the mould and then dried at ambient temperature for 72 h. The green samples were fired at 330 °C for 5 h, and then, the temperature was increased to 1000 °C with a heating rate of 1 °C/min to remove organic materials slowly. Finally, the samples were sintered in a muffle furnace at 1400–1650 °C for 4 h.

## Characterization

The microstructure of the porous alumina ceramics was observed using a scanning electronic microscope (SEM, JSM-6150 and JSM-7001F, JEOL, Japan). More than three hundred polystyrene spheres were measured by using an image particle analysis system (BT-1600, Bettersize Instruments Ltd., China), and the cell size was calculated by multiplying the original polystyrene sphere sizes by the linear shrinkage. The cell window size distribution was determined by mercury porosimetry (AutoPore IV 9500, Micromeritics Instrument Corp., America). The density and open porosity were measured in deionized water by the Archimedes method. The overall linear shrinkage of the sample was simply determined by the following equation:

$$\text{Linear shrinkage} = \left(\frac{l_g - l_s}{l_g}\right) \times 100\%$$

where $l_g$ and $l_s$ are the lengths of the mould and sintered sample, respectively.

## Compressive and bending strength tests

To obtain the compressive strength and bending strength of the porous alumina ceramics, the samples were loaded under displacement control mode by means of an electronic universal testing machine (AG-Xplus 100 kN, Shimadzu Corporation, Japan).

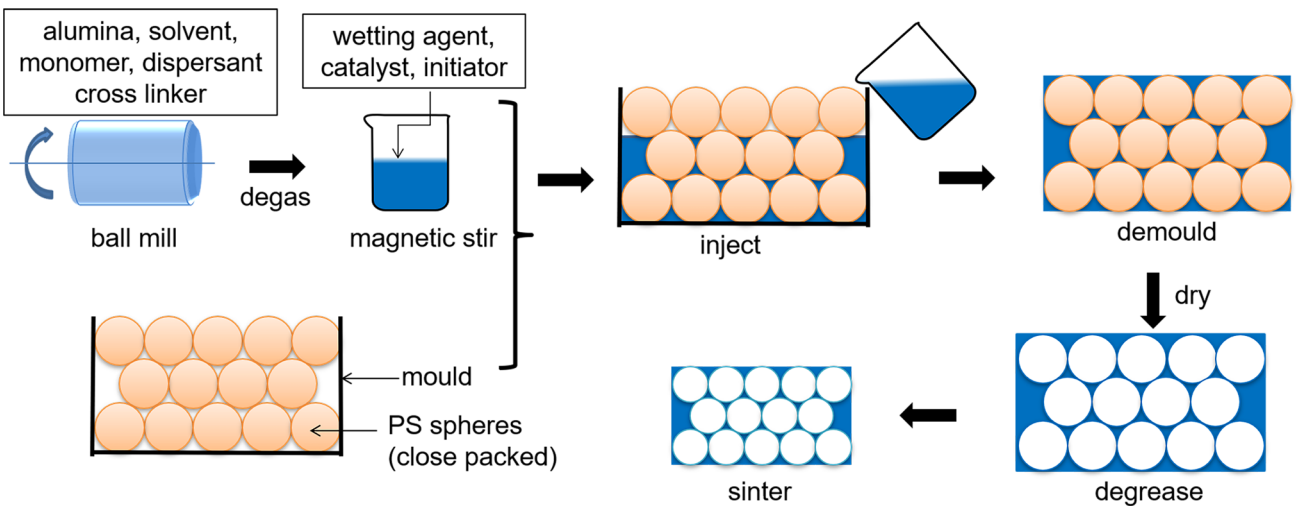


**Figure 1** Process flowchart for preparing porous alumina ceramics by a method that combines gel-casting and sacrificial templates.

**Table 1** The compositions of alumina slurries with different solid loading percentages

| Solid loading (vol%) | 30 | 35 | 40 | 45 | 50 |
|---|---|---|---|---|---|
| Alumina (g) | 36 | 43 | 50 | 60 | 70 |
| Deionized water (mL) | 21.2 | 20.2 | 18.9 | 18.5 | 17.7 |
| Dispersant (g) | 0.1462 | 0.1746 | 0.2030 | 0.2437 | 0.2843 |
| Monomer (g) | 3.4725 | 3.3012 | 3.1004 | 3.0315 | 2.8937 |
| Cross-linker (g) | 0.3473 | 0.3301 | 0.3100 | 0.3032 | 0.2894 |
| Wetting agent (μL) | 570 | 630 | 690 | 785 | 875 |
| Catalyst (μL) | 150 | 165 | 180 | 205 | 230 |
| Initiator (μL) | 1750 | 1935 | 2110 | 2405 | 2685 |

Compressive strength test was carried out with a loading rate of 0.5 mm/min and a span of 20 mm. While the bending strength was measured under a three-point bending mode, with a span of 24 mm and a loading rate of 0.5 mm/min. The samples were cut and ground into 10 mm × 20 mm × 20 mm and 10 mm × 10 mm × 40 mm for the compressive strength and bending strength tests, respectively. More than five samples were tested for both compressive strength and bending strength to obtain the average value along with the standard deviation.

## Results and discussions

### Pore structure of the porous alumina ceramics

Optical images of a representative porous alumina ceramic are shown in Fig. 2. The porous ceramic was prepared with 50% solid loading of the slurry and sintered at 1650 °C, and the median cell size was 796 μm. The sintered specimens achieved high porosity without cracks or deformations, which can be attributed to the low heating rate of 1 °C/min and heat preservation at 330 °C for 5 h. The spherical cells were regularly arranged, and the cell size was uniform. Meanwhile, the interconnection channels (cell window) between adjacent cells can be observed in Fig. 2b, indicating that the cells were open. This reveals that a method that combines sacrificial self-assembling polystyrene sphere templates and gel casting is effective for fabricating porous ceramics with uniform and regularly arranged pores.

Figure 3 shows the cell size distributions and morphologies of porous alumina ceramics prepared by polystyrene sphere templates of different sizes. The samples were prepared with 50% solid loading of the slurry and sintered at 1650 °C. As shown in the inset diagrams, large cells embedded in the alumina matrix were created by the removal of the polystyrene spheres. As a result, the cell size can be adjusted easily by changing the polystyrene sphere size. The porous alumina ceramics show a narrow cell size distribution, and the median cell size can be adjusted from 370 to 796 μm. In the following sections, if not mentioned, the porous alumina ceramics have a median cell size of 796 μm.

SEM micrographs of the fractured surface are presented in Fig. 4 to further study the pore structure of the porous alumina ceramics prepared using slurries of various solid loading percentages and sintered at 1650 °C. It can be found that the cell size is almost independent of the solid loading. However, the cell window size decreases with increasing solid loading. At high solid loadings, more alumina particles filled the interstices of the polystyrene spheres, resulting in a small window size.

Mercury porosimetry was used, which relies on the capillary effect to allow mercury to access the large cavities through narrow channels. In this manner, the diameter measured by mercury porosimetry corresponded to the cell window size [27, 28]. The window size distributions of the porous alumina ceramics that were fabricated using slurries of various solid loading percentages and sintered at 1650 °C are shown in Fig. 5. With increasing solid loading, the window size decreases. The window sizes of the porous alumina ceramics prepared using slurries of 30 vol% and 35 vol% solid loading are approximately 90 μm, and then, the window sizes decrease to 30–45 μm when using slurries of 40 vol% and 45 vol% solid loading. As the solid loading increases to 50 vol%, the window size decreases to 20 μm. In addition, the samples do not exhibit the bimodal window size distributions that other materials have reported [27, 28], which reveals that the cell wall has achieved a high degree of densification.

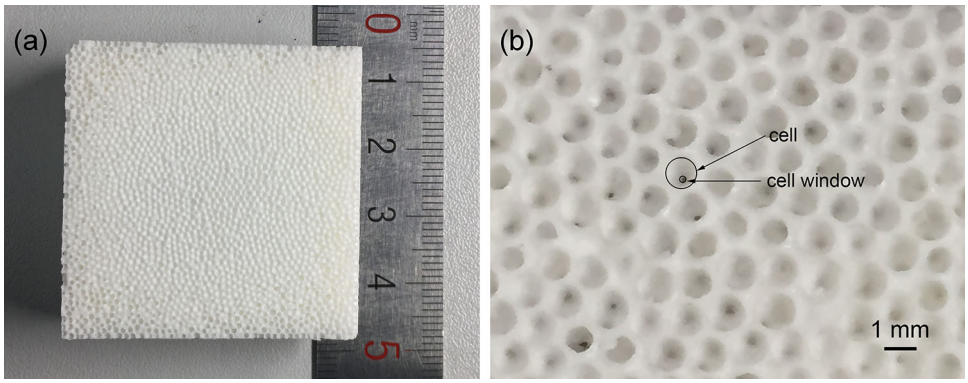


**Figure 2** Optical graphs of a representative porous alumina ceramic: **a** low magnification and **b** high magnification.

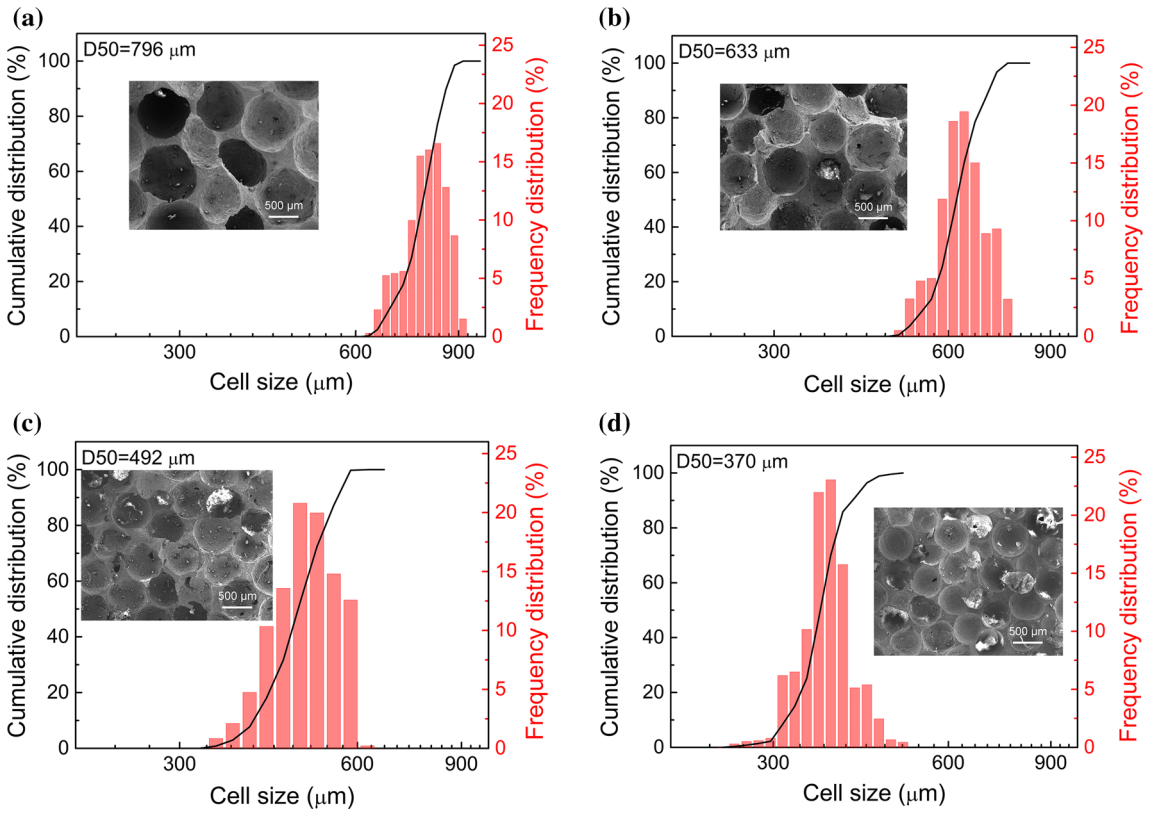


**Figure 3** Cell size distributions and cell morphologies of the porous alumina ceramics prepared by polystyrene spheres of different sizes.

As mentioned above, one of the advantages of gel casting is that it can achieve a high density of cell walls. Thus, the morphologies of the cell walls in the porous alumina ceramics sintered at various temperatures are shown in Fig. 6. Significant sintering stages can be distinguished at the various sintering temperatures. When sintered at 1400 °C, as shown in Fig. 6a, the sample presents a microstructure of high porosity and scarce development of sintering necks, which indicates a low cohesion of the particles and a low degree of sintering. At 1500 °C in Fig. 6b, the alumina ceramic is densified considerably, with increased grain size and the formation of sintering necks, indicating a middle stage of sintering. Upon further increasing the sintering temperature to 1600 °C, as shown in Fig. 6c, the grain size is increased significantly, but there are still pores between the grains at this final sintering stage. The cell wall had fully densified after sintering at 1650 °C, as shown in Fig. 6d. With respect to the fracture mode, it can be found that trans-granular fracture is the main mode when the samples were sintered at

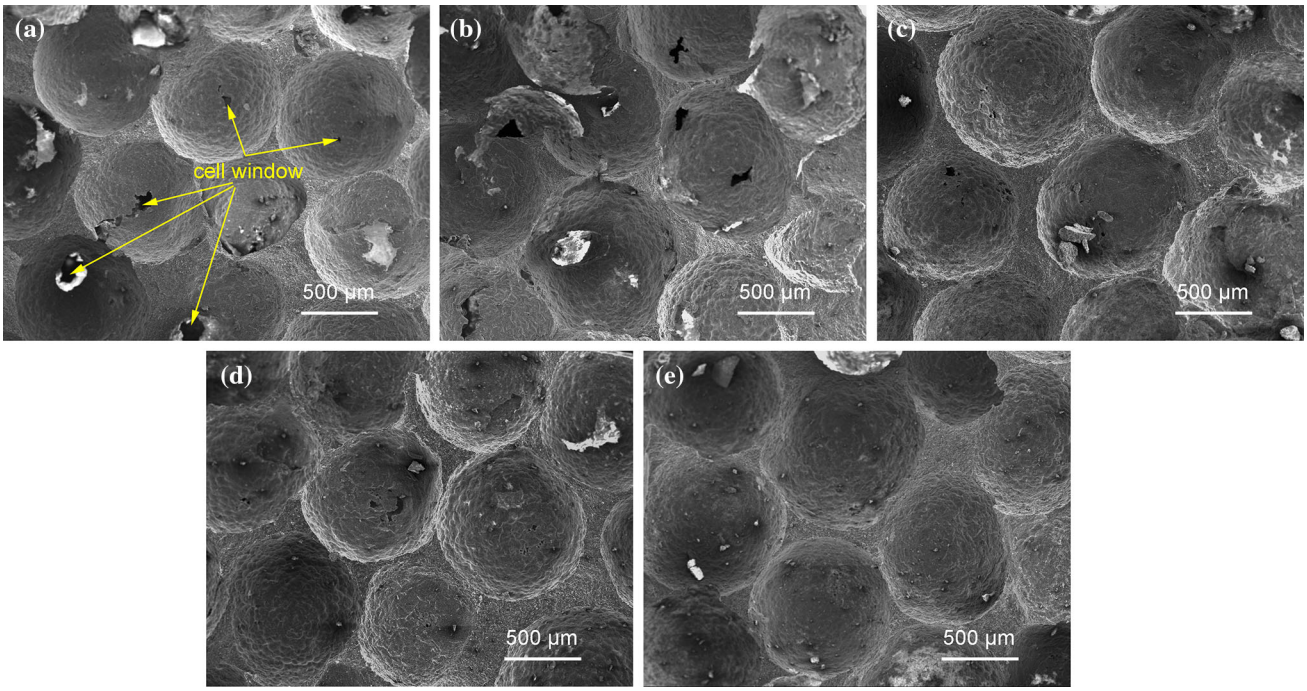


**Figure 4** SEM micrographs of the fractured surfaces of porous alumina ceramics sintered at 1650 °C and prepared with different solid loading percentage slurries: **a** 30 vol%, **b** 35 vol%, **c** 40 vol%, **d** 45 vol% and **e** 50 vol%.

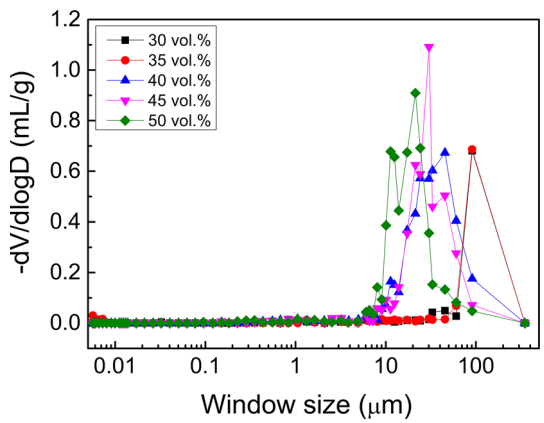


**Figure 5** Cell window size distributions of the porous alumina ceramics sintered at 1650 °C and fabricated using slurries of various solid loading percentages.

1400 °C and 1500 °C, as a result of its loose structure. However, with the increase in sintering temperature to 1600 °C and 1650 °C, the porous alumina ceramics with high density showed both inter-granular and trans-granular fractures, which are beneficial to the mechanical properties of the porous alumina ceramics.

## Physical properties of the porous alumina ceramics

As revealed above, the cells of the porous ceramics are controlled by the polystyrene spheres. Because the polystyrene spheres are regularly arranged, and the total volume is independent of the cell size, the cell size has almost no effect on the physical properties of the porous alumina ceramics. However, the solid loading percentage of the slurry influences the cell window size, and the sintering temperature affects the cell wall density. Thus, the influence of the solid loading and sintering temperature on the physical properties of the porous alumina ceramic are discussed below.

In Fig. 7a, both the sintering temperature and solid loading play important roles in the relative density of the porous alumina ceramics. With increasing sintering temperature from 1400 to 1650 °C, the relative density of the porous alumina ceramics shows an obvious increase. With increasing solid loading, the relative density of the porous ceramics increases at the sintering temperatures of 1400 °C and 1500 °C. As the sintering temperature was increased to 1600 °C and 1650 °C, all of the samples were almost completely sintered, and the effect of the solid

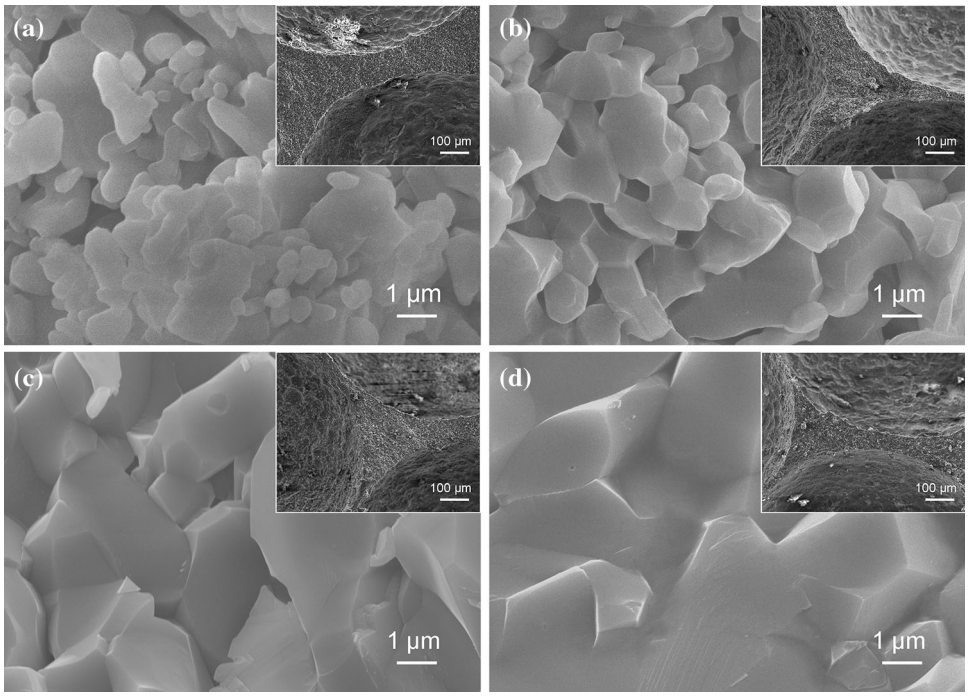


**Figure 6** SEM micrographs of the cell walls in the porous alumina ceramics prepared using slurries of 50 vol% solid loading and sintered at various temperatures: **a** 1400 °C, **b** 1500 °C, **c** 1600 °C and **d** 1650 °C.

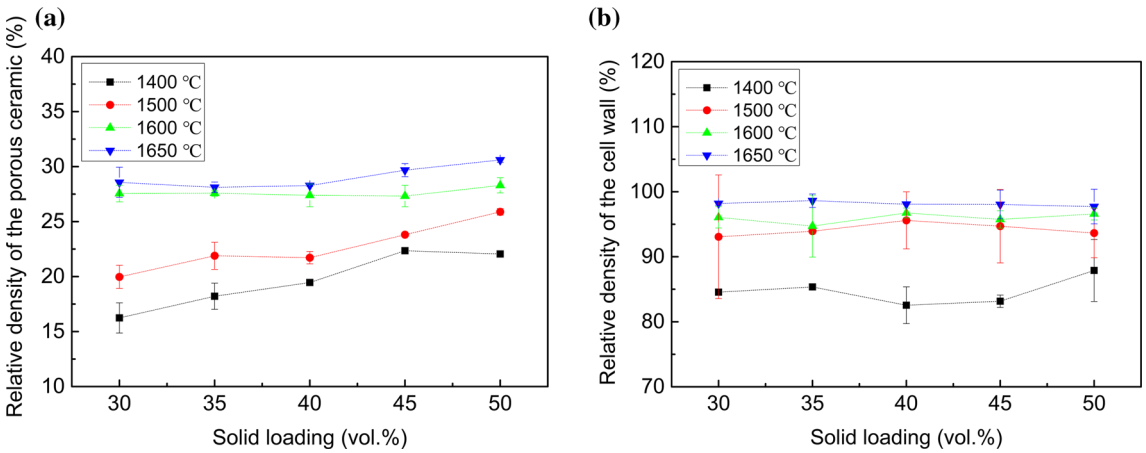


**Figure 7** Effects of the sintering temperature and solid loading percentage on the relative density of **a** the porous alumina ceramics and **b** the cell walls.

loading on the relative density of the porous ceramics is small. Due to the smaller window size, the relative density of the porous ceramics prepared with higher solid loading is slightly larger.

It is worth mentioning that because polystyrene spheres are close-packed, the theoretical relative density of the polystyrene spheres is 74%, and the relative density of the porous alumina ceramics should be 26%. It can be easily understood that the relative density of the porous ceramics is lower than the theoretical value due to the incomplete sintering at 1400 °C and 1500 °C. However, when sintered at 1600 °C and 1650 °C, the samples achieve a higher relative density than the theoretical value. This may be caused by the possible existence of imperfect packing of the polystyrene spheres. Ultra-sound or tapping may further enhance the packing ability of the polystyrene sphere template, modifying the final microstructure and increase the packing density.

As for the relative density of the cell walls, shown in Fig. 7b, the sintering temperature rather than the solid loading percentage played a decisive role. With an increase in the sintering temperature from 1400 to 1650 °C, the relative density of the cell walls increases

significantly from approximately 85–98%, consistent with the results in Fig. 6. Moreover, the dense ceramics without polystyrene sphere templates were prepared by gel casting and sintered at 1650 °C, and its relative density is 98.6%, nearly the same as that of the cell wall of the porous ceramics. This proves that the cells in porous alumina ceramics should be open. The highly dense cell walls will make a substantial contribution to the mechanical properties.

Figure 8 shows the overall linear shrinkage of the porous alumina ceramics prepared using slurries of various solid loading percentages and sintered at various temperatures for 4 h. It is obvious that the sintering temperature is the main factor for determining the linear shrinkage of the porous alumina ceramics. With increasing sintering temperature from 1400 to 1600 °C, the linear shrinkage rapidly increases from 6% to approximately 18%. With a further increase in the sintering temperature to 1650 °C, the linear shrinkage of the porous alumina ceramics increased slightly to approximately 19%, in accordance with the final sintering stage. Additionally, with an increase in the solid loading percentage, the linear shrinkage shows a slight downward trend. This slight decrease in the linear shrinkage may be caused by the increased density of the green body when the solid content increases.

## Mechanical properties of the porous alumina ceramics

The porous alumina ceramics prepared using various sizes of polystyrene spheres, solid loading percentages and sintering temperatures, all have various cell sizes, window sizes and cell wall densities, resulting in different mechanical properties.

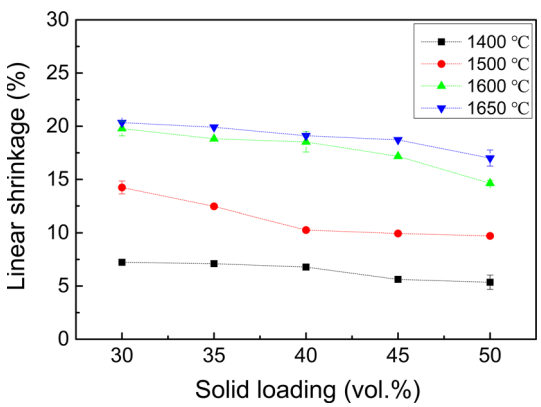


**Figure 8** Effects of the sintering temperature and solid loading percentage on the linear shrinkage of the porous alumina ceramics.

Figure 9a shows the influences of the solid loading percentage and sintering temperature on the bending strength of the porous alumina ceramics. With increasing solid loading, the bending strength of the porous alumina ceramics increases. With increasing sintering temperature, the bending strength shows a significant and continuous increase. Taking the solid loading of 30 vol% and 50 vol% as examples, the bending strength is 1.1 MPa and 3.6 MPa after sintering at 1400 °C, respectively, and significantly increases to 13.3 MPa and 19.2 MPa when the sintering temperature was increased to 1650 °C, respectively. It can be concluded that the sintering temperature has a larger influence on the bending strength than does the solid loading percentage. Meanwhile, the cell size has little influence on the bending strength, as shown in Table 2, and the highest bending strength of the porous alumina ceramics in this work is approximately 19 MPa. Thus, except for porosity, the density of the cell wall and the cell window size are the main factors that affect the bending strength of porous alumina ceramics [29].

The compressive strength of the porous alumina ceramic is shown in Fig. 9b. With increasing sintering temperature, the compressive strength increases significantly due to densification of the cell walls. For a constant sintering temperature, with increasing solid loading percentage, the compressive strength of the porous alumina ceramics increases slowly when the solid loading is in the range of 30–40 vol% and then increases rapidly as the solid loading increases to 45–50 vol%. For the sample with a solid loading of 50 vol% and a sintering temperature of 1650 °C, the compressive strength is as high as 21 MPa. Moreover, as shown in Table 2, with decreases in the cell size, the compressive strength shows an increasing trend. The maximum compressive strength of 28 MPa was obtained when the pore size decreased to 370 μm, in this work. This indicates that the cell wall density, cell window size and cell size are all important influencing factors for the compressive strength.

Generally, the mechanical strength of porous ceramics increases with decreasing pore size when the porosities are close to each other [23, 30–32]. This is caused by size effect [33]. In this work, the larger the pore size, the thicker the cell wall. Brittle specimens with big cells fail at low stresses simply because

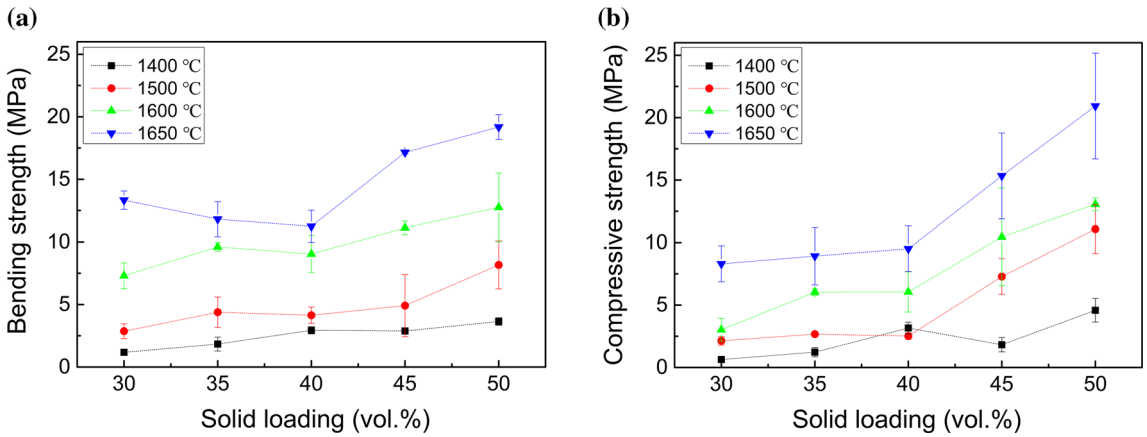


**Figure 9** Effects of the sintering temperature and solid loading percentage on mechanical properties of the porous alumina ceramics: **a** bending strength and **b** compressive strength.

**Table 2** The influence of the cell size on the strength of the porous alumina ceramics sintered at 1650 °C with a solid loading of 50 vol%

| Cell size (D50, μm) | Polystyrene sphere size (μm) | The number of samples | Relative density (%) | Bending strength (MPa) | Compressive strength (MPa) |
|---|---|---|---|---|---|
| 796 | 960 | 5 | 30.61 (± 0.23) | 19.18 (± 0.99) | 20.93 (± 4.24) |
| 633 | 750 | 8 | 31.48 (± 0.05) | 16.74 (± 0.79) | 23.40 (± 3.05) |
| 492 | 570 | 6 | 30.54 (± 0.17) | 18.92 (± 2.37) | 27.72 (± 1.18) |
| 370 | 430 | 6 | 31.94 (± 0.39) | 18.94 (± 0.04) | 28.01 (± 0.29) |

it is more probable that they contain a large pre-existing crack. However, as presented in Table 2, the bending strength of porous alumina ceramics is independent of the cell size, while the compressive strength follows the general rules. In the bending test, the sample is mainly subjected to tensile stress, and when the crack reaches the critical dimension, it will destabilize and expand, causing the sample to break. Therefore, the bending strength is determined by the maximum crack size. The largest crack in the cell wall is the cell window, and the cell size has almost no influence on the cell window, as shown in the inset of Fig. 3. So, with the decrease in cell size, the bending strength of porous alumina ceramics almost remains the same, whereas when the sample is under compressive stress, the propagation of crack is slow, and the compressive strength is determined by the average size of crack. As a result, with decreasing cell size, the average crack size decreases, causing an increase in the compressive strength.

Figure 10 presents the bending strength and compressive strengths of macro-porous alumina ceramics made by various methods with pore sizes greater than 100 μm. With increasing relative density, both the bending strength and compressive strengths of the porous ceramics show an increasing trend. Compared with that of samples of the same density that were made by other authors, the compressive strength of the sample in this work, marked by a star, is at least 74% higher. This is ascribed to the improvements of the microstructure in the sample of this work. On the one hand, regularly arranged cells and fully dense cell walls are the dominant factors in the improvement of the mechanical properties. On the other hand, the smaller window size and more homogeneous cell size distribution further contribute to the improvement of the mechanical properties.

## Conclusion

Macro-porous alumina ceramics with both high porosity and high strength were prepared by a combination of the gel-casting and sacrificial template methods. The resulting high cell wall density and regularly arranged pores confer high mechanical

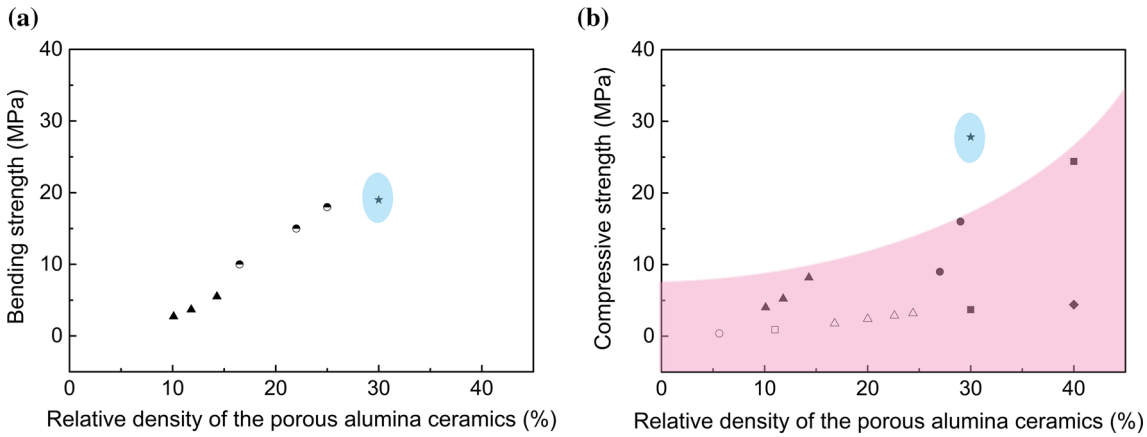


**Figure 10** Bending strength and compressive strengths of porous alumina ceramics made by various methods; data marked by a star are the porous alumina ceramic of this work. Others were obtained from Refs. [1, 15, 19, 26, 30, 34–36]: circle, Ref. [1]; square, Ref. [15]; filled square, Ref. [19]; triangle, Ref. [26]; filled circle, Ref. [30]; diamond, Ref. [34]; filled triangle, Ref. [35]; and half open circle, Ref. [36].

strength to the porous ceramics. The results show that the sintering temperature, polystyrene sphere size and solid loading percentage of the alumina slurry influence the density of the cell wall, cell size and cell window size, respectively. With increasing sintering temperature and solid loading percentage, the strength of the porous alumina ceramic shows an increasing trend. The porous alumina ceramic achieves the highest mechanical strength when prepared with a 50 vol% solid loading slurry and sintered at 1650 °C. Here, the relative density of the porous ceramic, relative density of the cell wall and linear shrinkage are 30%, 98% and 17%, respectively. Moreover, with the decrease in the cell size to about 370 μm, the compressive strength increases to 28 MPa, which is at least 74% higher than that of the reported porous alumina ceramics that have a random structure. This process is also advantageous for making high-strength porous ceramics of complicated shapes and large sizes.

## Acknowledgements

This work was supported by the National Natural Science Foundation of China (51872033, 51732007, 51472047), the National Key R&D Program of China (2017YFB0310300) and the fund of the State Key Laboratory of Advanced Technologies for Comprehensive Utilization of Platinum Metals (SKL-SPM-201505 and SKL-SPM-201506).

## References

[1] Soh E, Kolos E, Ruys AJ (2015) Foamed high porosity alumina for use as a bone tissue scaffold. Ceram Int 41:1031–1047

[2] Rambo CR, Andrade T, Fey T, Sieber H, Martinelli AE, Greil P (2008) Microcellular $Al_2O_3$ ceramics from wood for filter applications. J Am Ceram Soc 91:852–859

[3] Han L, Li F, Deng X, Wang J, Zhang H, Zhang S (2017) Foam-gelcasting preparation, microstructure and thermal insulation performance of porous diatomite ceramics with hierarchical pore structures. J Eur Ceram Soc 37:2717–2725

[4] Ismail AK, Abdullah MZ, Zubair M, Jamaludin AR, Ahmad ZA (2016) Effect of ceramic coating in combustion and cogeneration performance of $Al_2O_3$ porous medium. J Energy Inst 89:81–93

[5] Mueller KT, Waters O, Bubnovich V, Orlovskaya N, Chen R-H (2013) Super-adiabatic combustion in $Al_2O_3$ and SiC coated porous media for thermoelectric power conversion. Energy 56:108–116

[6] Liu PS, Chen GF (2014) Applications of porous ceramics. In: Porous materials. Butterworth-Heinemann, Oxford, pp 303–344

[7] Ohji T, Fukushima M (2013) Macro-porous ceramics: processing and properties. Int Mater Rev 57:115–131

[8] Staub D, Meille S, Le Corre V, Rouleau L, Chevalier J (2016) Identification of a damage criterion of a highly porous alumina ceramic. Acta Mater 107:261–272

[9] Manoj Kumar BV, Kim YW (2010) Processing of polysiloxane-derived porous ceramics: a review. Sci Technol Adv Mater 11:044303

[10] Yang Z, Yu J, Li C, Zhong Y, Xuan W, Ren Z, Wang Q, Dai Y, Wang H (2015) Preparation of textured porous $Al_2O_3$ceramics by slip casting in a strong magnetic field and its mechanical properties. Cryst Res Technol 50:645–653

[11] Ebrahimpour O, Dubois C, Chaouki J (2014) Fabrication of mullite-bonded porous SiC ceramics via a sol–gel assisted in situ reaction bonding. J Eur Ceram Soc 34:237–247

[12] Liu R, Li Y, Wang C-A, Tie S (2014) Fabrication of porous alumina–zirconia ceramics by gel-casting and infiltration methods. Mater Des 63:1–5

[13] Salomão R, Fernandes L (2017) Porous co-continuous mullite structures obtained from sintered aluminum hydroxide and synthetic amorphous silica. J Eur Ceram Soc 37:2849–2856

[14] Studart AR, Gonzenbach UT, Tervoort E, Gauckler LJ (2006) Processing routes to macroporous ceramics: a review. J Am Ceram Soc 89:1771–1789

[15] Jamaludin AR, Kasim SR, Abdullah MZ, Ahmad ZA (2016) Physical, mechanical, and thermal properties improvement of porous alumina substrate through dip-coating and re-sintering procedures. Ceram Int 42:7717–7729

[16] Huang K, Li Y, Li S, Xiang R (2016) Preparation and properties of alumina foams via thermally induced foaming of molten D-glucose monohydrate. J Porous Mater 24:121–128

[17] Yang Y, Shimai S, Sun Y, Dong M, Kamiya H, Wang S (2013) Fabrication of porous $Al_2O_3$ ceramics by rapid gelation and mechanical foaming. J Mater Res 28:2012–2016

[18] Deng X, Ran S, Han L, Zhang H, Ge S, Zhang S (2017) Foam-gelcasting preparation of high-strength self-reinforced porous mullite ceramics. J Eur Ceram Soc 37:4059–4066

[19] Tulliani JM, Lombardi M, Palmero P, Fornabaio M, Gibson LJ (2013) Development and mechanical characterization of novel ceramic foams fabricated by gel-casting. J Eur Ceram Soc 33:1567–1576

[20] Deville S (2008) Freeze-casting of porous ceramics: a review of current achievements and issues. Adv Eng Mater 10:155–169

[21] Chen R, Wang C-A, Huang Y, Ma L, Lin W (2007) Ceramics with special porous structures fabricated by freeze-gelcasting: using tert-Bbutyl alcohol as a template. J Am Ceram Soc 90:3478–3484

[22] Zhao H, Li L, Ding S, Liu C, Ai J (2018) Effect of porous structure and pore size on mechanical strength of 3D-printed comby scaffolds. Mater Lett 223:21–24

[23] Liu R, Wang C-A (2013) Effects of mono-dispersed PMMA micro-balls as pore-forming agent on the properties of porous YSZ ceramics. J Eur Ceram Soc 33:1859–1865

[24] Ortiz-Landeros J, Contreras-García ME, Pfeiffer H (2008) Synthesis of macroporous $ZrO_2$–$Al_2O_3$ mixed oxides with mesoporous walls, using polystyrene spheres as template. J Porous Mater 16:473–479

[25] Waterhouse GIN, Chen W-T, Chan A, Jin H, Sun-Waterhouse D, Cowie BCC (2015) Structural, optical, and catalytic support properties of $\gamma$-$Al_2O_3$ inverse opals. J Phys Chem C 119:6647–6659

[26] Yu JY, Sun XD, Li Q, Li XD (2008) Preparation of $Al_2O_3$ and $Al_2O_3$–$ZrO_2$ ceramic foams with adjustable cell structure by centrifugal slip casting. Mater Sci Eng, A 476:274–280

[27] Talou MH, Camerucci MA (2015) Processing of porous mullite ceramics using novel routes by starch consolidation casting. J Eur Ceram Soc 35:1021–1030

[28] Yin L, Zhou X, Yu J, Wang H (2016) Preparation of silicon nitride foam with three-dimensional interconnected pore structure. Mater Des 89:620–625

[29] Yang XJ, Li B, Zhang CR, Wang SQ, Liu K, Zou CR (2016) Fabrication and properties of porous silicon nitride wave-transparent ceramics via gel-casting and pressureless sintering. Mater Sci Eng, A 663:174–180

[30] Meille S, Lombardi M, Chevalier J, Montanaro L (2012) Mechanical properties of porous ceramics in compression: on the transition between elastic, brittle, and cellular behavior. J Eur Ceram Soc 32:3959–3967

[31] Miled K, Sab K, Le Roy R (2007) Particle size effect on EPS lightweight concrete compressive strength: experimental investigation and modelling. Mech Mater 39:222–240

[32] Liu D-M (1997) Influence of porosity and pore size on the compressive strength of porous hydroxyapatite ceramic. Ceram Int 23:135–139

[33] Gibson LJ, Ashby MF (1997) Cellular solids structure and properties, 2nd edn. Cambridge University Press, Cambridge

[34] Su Z, Xi X, Hu Y, Fei Q, Yu S, Li H, Yang J (2014) A new $Al_2O_3$ porous ceramic prepared by addition of hollow spheres. J Porous Mater 21:601–609

[35] Potoczek M (2008) Gelcasting of alumina foams using agarose solutions. Ceram Int 34:661–667

[36] Mao X, Shimai S, Wang S (2008) Gelcasting of alumina foams consolidated by epoxy resin. J Eur Ceram Soc 28:217–222